Somatostatin Receptor 1 Selective Analogues: 3. Dicyclic Peptides

Jean E. Rivier,*,† Dean A. Kirby,† Judit Erchegyi,† Beatrice Waser,‡ Véronique Eltschinger,‡ Renzo Cescato,‡ and Jean Claude Reubi‡

The Clayton Foundation Laboratories for Peptide Biology, The Salk Institute, 10010 N. Torrey Pines Road, La Jolla, California 92037, and Division of Cell Biology and Experimental Cancer Research, Institute of Pathology, University of Berne, Berne, Switzerland

Received June 18, 2004

The binding affinity of short chain somatostatin (SRIF) analogues at the five human SRIF receptors (sst) was determined to identify sterically constrained somatostatin receptor subtype 1 (sst_1) selective scaffolds. Des-AA^{1,2,4,13}-[D-Trp^8]SRIF (**2**) retained high binding affinity at all receptors but sst_1, Des-AA^{1,2,4,5}-[D-Trp^8]SRIF (**3**) at sst_4 and sst_5, and Des-AA^{1,2,4,5,13}-[D-Trp^8]-SRIF (**4**) at sst_2 and sst_4 (AA = amino acid). Des-AA^{1,2,4,12,13}-[D-Trp^8]SRIF (**6**) was potent and sst_4-selective (>25-fold); Des-AA^{1,2,5,12,13}-[D-Trp^8]SRIF (**7**) and Des-AA^{1,2,4,5,12,13}-[D-Trp^8]-SRIF (**9**, ODT-8) were most potent at sst_4 and moderately potent at all other receptors. Dicyclic SRIF agonists of the sst_1-selective Des-AA^{1,5}-[Tyr^2,D-Trp^8,IAmp^9]SRIF, (**14**, sst_1 IC_{50} = 14 nM) were prepared in which a lactam bridge introduced additional conformational constraint (IAmp = 4-(*N*-isopropyl)-aminomethylphenylalanine). Cyclo(7−12)Des-AA^{1,5}-[Tyr^2,Glu^7,D-Trp^8,IAmp^9,-hhLys^{12}]SRIF (**31**) (sst_1 IC_{50} = 16 nM) and cyclo(7−12) Des-AA^{1,2,5}-[Glu^7,D-Trp^8,IAmp^9,m-I-Tyr^{11},hhLys^{12}]SRIF (**45**) (sst_1 IC_{50} = 6.1 nM) had equal or improved affinities over that of the parent **14**. Binding affinity was decreased in all other cases with alternate bridging constraints such as cyclo (6−11), cyclo (6−12), and cyclo (7−11). Compound **45** is an agonist (EC_{50} = 8.8 nM) in the adenylate cyclase assay.

Introduction

The cyclic peptide hormone somatostatin (SRIF), first isolated from ovine hypothalamus in 1973,[1] characterized,[2] and synthesized[3] in our laboratories, has since been found to modulate numerous actions in the body that are mediated by at least five SRIF receptors (sst_{1-5}).[4−10] Among its most important roles, SRIF is an inhibitor of growth hormone (GH),[2] glucagon, and insulin secretions.[11]

The aim of this study was to use the available structure−activity relationships (SAR) of sst_1-selective analogues for the design of sst_1-selective constrained analogues amenable to NMR investigation for the determination of the sst_1 pharmacophore[12] and to generate compounds with high in vivo potency and either agonist or antagonist activity for mechanistic studies. An updated review of sst_1 receptor localization and function as well as a rationale for the need of sst_1-selective ligands is given in the preceding paper.[13]

The early observation that shortened chain analogues of SRIF, both peptidic as well as nonpeptide mimetics,[14−17] retained significant biological activities[18,19] ultimately led to the development of several drugs and drug candidates. These include octreotide[20] and derivatives such as Octreoscan, vapreotide, and lanreotide and, more recently, SOM230[21] and KE108.[22] Several reviews describe the use of these analogues in the management of numerous pathological conditions and cancer treatments.[14,17,23−27] Because these early analogues had been tested for their relative potencies in inhibiting GH, insulin, and glucagon secretions and shown in some cases to be selective,[19,28−31] we measured their binding affinity for the five sst (Table 1).

In addition, highly constrained analogues that are preferred as their solution conformations will help define the structure of the pharmacophore using NMR and computer modeling techniques.[32−39] In our quest for novel scaffolds that would lead to ligands with high-binding affinity and sst selectivity, we synthesized a series of shortened, presumably more structurally stable, SRIF analogues (Table 1). This design strategy for a constrained backbone motif has precedence in the design of ODT-8 (Figure 1B),[18,19] octreotide (Figure 1C),[20] and CH-275 (Figure 1D)[40] as compared to SRIF (schematically depicted in Figure 1A). The ODT-8 scaffold originated from the observation that, in an alanine scan of SRIF, substitutions at positions 4, 5, 10, 12, and 13 resulted in analogues essentially equipotent to SRIF whereas substitutions at positions 6, 7, 8, 9, and 11 resulted in significantly less potent analogues (100-fold loss).[18,19] This suggested that double deletions such as Des-AA^{4,13} and Des-AA^{4,5,12,13} may conserve the structural features of the postulated β-turn responsible for activity. This was indeed the case as shown by us[18,19] and confirmed later by others with the octreotide scaffold (Figure 1C)[20] and the work by the Merck group headed by R. Hirschmann, which made the seminal observation that the π-stacking of the phenylalanine side chains at positions 6 and 11 of SRIF may have a structure-stabilizing role[32,33] critical for the propitious alignment of the side chains of residues 7−10 in a bioactive conformation. The scaffold of CH-275 was first identified by Sarantakis et al.[41] who observed that Des-Ala^1,Gly^2,Asn^5-SRIF, {H-cyclo[Cys^3-Lys^4-Phe^6-Phe^7-Trp^8-

* Author to whom correspondence should be addressed. Phone: (858) 453-4100. Fax: (858) 552-1546. E-mail: Jrivier@salk.edu
† The Salk Institute.
‡ University of Berne.

10.1021/jm049519m CCC: $30.25
Published on Web 12/23/2004

Table 1. Effect of SRIF Ring Shortening on Binding Affinity

	compound	cycle size[e]	HPLC[a]	CZE[b]	MS[e] M calc.	MS[e] $[M + H]^+$	IC_{50} (nM)[d] sst_1	sst_2	sst_3	sst_4	sst_5	relative potencies GH (1)	insulin (1)	glucagon (1)
1	SRIF[f]		98	93	1636.72	1637.7	1.9 ± 0.53 (5)	0.7 ± 0.2 (5)	3.3 ± 1.7 (4)	1.6 ± 0.8 (4)	10 ± 4.4 (4)	100	100	100
2	Des-AA[1,2,4,13]-[D-Trp[8]]SRIF	32	98	>98	1293.53	1294.7	112 (127, 96)	5.0 (3.5, 6.5)	11 (15, 7.6)	1.4 (1.6, 1.2)	9.5 (8, 11)	8	75	8
3*	Des-AA[1,2,4,5]-[D-Trp[8]]SRIF	32	95	98	1266.52	1267.6	79 (61, 97)	28 (25, 30)	222 (160, 284)	3.3 (2.1, 4.5)	8.6 (9.2, 8.0)	110	700	<1
4	Des-AA[1,2,4,5,13]-[D-Trp[8]]SRIF	29	98	98	1179.49	1180.5	197 ± 26 (4)	1.9 ± 0.5 (4)	52 ± 15 (3)	1.0 ± 0.2 (4)	43 ± 12 (4)			
5*	Des-AA[1,4,5,13]-[Tyr[2],D-Trp[8],IAmp[9]]SRIF	29	95	98	1432.60	1433.4	720 (890, 550)	> 1K (2)	445 (600, 290)	> 1K (2)	> 1K (2)			
6	Des-AA[1,2,4,12,13]-[D-Trp[8]]SRIF	29	93	93	1192.48	1193.5	59 ± 23 (4)	95 ±16 (4)	189 ± 43 (3)	1.2 ± 0.3 (4)	31 ± 11 (3)	<1	72	<1
7	Des-AA[1,2,5,12,13]-[D-Trp[8]]SRIF	29	>98	>98	1206.53	1207.5	5.3 ± 1.6 (3)	15 ± 2.3 (4)	39 ± 15 (4)	0.6 ± 0.03 (3)	13 ± 2.7 (4)	15	310	115
8	Des-AA[1,2,5,12,13]-[D-Trp[8],IAmp[9]]SRIF	29	>98	>98	1296.58	1297.1	189 ± 31 (3)	> 1K (3)	789 ± 232 (3)	932 ± 125 (3)	> 1K (3)			
9*	Des-AA[1,2,4,5,12,13]-[D-Trp[8]]SRIF (ODT-8)	26	95	98	1078.44	1079.2	27± 3 (4)	41 ±9 (6)	13 ± 3 (4)	1.8 ± 0.7 (4)	46 ± 27 (3)	4	45	7
10	Des-AA[1,2,4,5,6,12,13]-[D-Trp[8]]SRIF	23	96	97	931.37	932.3	> 1K (2)	531 (503, 558)	> 1K (2)	229 (242, 215)	> 1K (2)			
11	Des-AA[1,2,4,5,11,12,13]-[D-Trp[8]]SRIF	23	96	95	931.37	932.4	> 1K (2)	598 (333, 862)	> 1K (2)	> 1K (2)	> 1K (2)	0.07	<1	<1
12	Des-AA[1,2,4,5,10,12,13]-[D-Trp[8]]SRIF	23	>98	98	977.39	978.3	> 1K (2)	> 1K (2)	905 (657, 1153)	786 (490, 1082)	> 1K (2)	<0.01	<1	<1
13	Des-AA[1,4,5,6,12,13]-[Tyr[2],D-Trp[8],IAmp[9]]SRIF	23	96	98	1184.48	1185.5	> 1K (2)	> 1K (2)	> 1K (2)		> 1K (2)			

[a] Percent purity determined by HPLC using buffer system: A = TEAP (pH 2.5) and B = 60% CH_3CN/40% A with a gradient slope of 1% B/min, at flow rate of 0.2 mL/min on a Vydac C_{18} column (0.21 cm × 15 cm, 5-μm particle size, 300 Å pore size). Detection at 214 nm. [b] CZE was done using a Beckman P/ACE System 2050 controlled by an IBM Personal System/2 model 50Z and using a ChromJet integrator. Field strength of 15 kV at 30 °C, mobile phase: 100 mM sodium phosphate (85:15, H_2O/CH_3CN) pH 2.50, on a Supelco P175 capillary (363 μm o.d. × 75 μm i.d. × 50 cm length). Detection at 214 nm. [c] The calculated *m/z* of the monoisotope compared with the observed $[M + H]^+$ monoisotopic mass. [d] The IC_{50} values (nM) were derived from competitive radioligand displacement assays reflect the affinities of the analogues for the cloned somatostatin receptors using the nonselective ^{125}I-[Leu[8],D-Trp[22],Tyr[25]]SRIF-28, as the radioligand. Mean value ± SEM when $N \geq 3$ (shown in parentheses). Otherwise, mean with single values in parentheses. [e] Number of atoms in the cycle. [f] SRIF = H-Ala[1]-Gly[2]-c[Cys[3]-Lys[4]-Asn[5]-Phe[6]-Phe[7]-Trp[8]-Lys[9]-Thr[10]-Phe[11]-Thr[12]-Ser[13]-Cys[14]]-OH. * Described in part 1, reference 1.

Figure 1. Illustration of established and proposed scaffolds for the design of sst_1-selective ligands.

Lys[9]-Thr[10]-Phe[11]-Thr[12]-Ser[13]-Cys[14]]-OH}, was a potent and selective inhibitor of insulin and not glucagon.

Here, we followed two distinct approaches for the design of conformationally constrained and sst-selective SRIF analogues. In the first one, analogues that had been synthesized and tested more than 20 years ago for their ability to inhibit GH, insulin, and glucagon in the rat were now tested for their ability to bind to the five sst. In the second one, a strategy similar to that carried out by the Merck group[33,42] whereby, starting with the CH-275 scaffold[40] (Figure 1D), an additional bridge between residues 7 and 12 (SRIF nomenclature, Figure 1E, Table 2) that is compatible with retention of high affinity for sst_1 was identified. It was hypothesized that deletion of the cystine-containing ring shown in Figure 1E in a manner shown in Figure 1F may result in a shorter sst_1-selective analogue.

Results and Discussion

Synthesis. All of the analogues shown in Tables 1 and 2 were synthesized either manually or automatically on a chloromethylated resin using the Boc strategy and *N*,*N*′-diisopropylcarbodiimide (DIC) for amide bond formation (Boc = *tert*-butoxycarbonyl). The side chains of the internal bridgeheads were protected with the base-sensitive OFm and Fmoc groups (OFm = γ-9-fluorenylmethyl ester, Fmoc = 9-fluorenylmethoxycarbonyl). Cyclization was achieved after piperidine treatment of the fully protected peptide resin using BOP as described originally by Felix et al.[43] or TBTU (BOP = (benzotriazol-1-yloxy)tris(dimethylamino)phosphonium hexafluorophosphate, TBTU = 2-(1H-benzotriazol-1-yl)-tetramethyluronium tetrafluoroborate). The peptide resins were treated with hydrogen fluoride in the presence of scavengers to liberate the fully deblocked, lactam-bridged analogues. Cyclization of the cysteines was mediated by iodine in an acidic milieu.[44] Purification was carried out using multiple high-performance liquid chromatography (HPLC) steps,[45] and characterization by HPLC,[45] capillary zone electrophoresis,[46] and mass spectrometry. The measured masses obtained using matrix-assisted laser desorption ionization mass spectrometry (MALDI-MS) were as expected. Because **2**−**4**, **6**, and **9**−**12**, made on solid phase, had been purified using partition chromatography or countercurrent distribution, it was important to check first whether they had retained their chemical integrity upon standing more than 25 years in a freezer and most importantly whether they were indeed the expected compounds. It was very rewarding to find out that these analogues, the purification of which had been monitored by thin-layer chromatography, were stable, had the expected molecular weights, and were of high purity (determined by HPLC and capillary zone electrophoresis

Table 2. Effect of Added Cyclic Constraints to CH-275 on Binding Affinity and Selectivity[f,g]

	compound	cycle size[e]	HPLC[a]	CZE[b]	MS[c] M calc.	MS[c] $[M+H]^+$	IC_{50}[d] (nM) sst$_1$	sst$_2$	sst$_3$	sst$_4$	sst$_5$
14	Des-AA^{1,5}-[Tyr^2,D-Trp^8,IAmp^9]SRIF CH-288		97	97	1647.73	1648.8	14 ± 2.7 (8)	>1K (6)	>1K (7)	>1K (6)	>1K (7)
15	cyclo(6−11) Des-AA^{1,5}-[Tyr^2,Glu^6,D-Trp^8,IAmp^9,Dab^{11}]SRIF	22	98	97	1565.68	1566.8	597 (800, 393)	>1K (2)	>1K (2)	>1K (2)	>1K (2)
16	cyclo(6−11) Des-AA^{1,5}-[Tyr^2,D-Glu^6,D-Trp^8,IAmp^9,D-Dab^{11}]SRIF	22	98	90	1565.68	1566.6	>1K (2)	>1K (2)	>1K (2)	>1K (2)	>1K (2)
17	cyclo(6−11) Des-AA^{1,5}-[Tyr^2,Glu^6,D-Trp^8,IAmp^9,Lys^{11}]SRIF	24	94	97	1592.72	1593.8	>1K (2)	>1K (2)	>1K (2)	>1K (2)	>1K (2)
18	cyclo(6−12) Des-AA^{1,5}-[Tyr^2,Asp^6,D-Trp^8,IAmp^9,Dap^{12}]SRIF	23	95	96	1583.67	1584.6	>1K (2>	>1K (2)	>1K (2)	>1K (2)	>1K (2)
19	cyclo(6−12) Des-AA^{1,5}-[Tyr^2,Glu^6,D-Trp^8,IAmp^9,Dab^{12}]SRIF	25	98	>98	1610.71	1613.4	104 (60, 148)	>1K (2)	>1K (2)	>1K (2)	>1K (2)
20	cyclo(6−12) Des-AA^{1,5}-[Tyr^2,Glu^6,D-Trp^8,IAmp^9,Lys^{12}]SRIF	27	98	93	1637.74	1638.7	208 (250, 166)	>1K (2)	>1K (2)	>1K (2)	>1K (2)
21	cyclo(7−11) Des-AA^{1,5}-[Tyr^2,Glu^7,D-Trp^8,IAmp^9,Dab^{11}]SRIF	19	93	90	1564.69	1565.7	>1K (2)	>1K (2)	>1K (2)	>1K (2)	>1K (2)
22	cyclo(7−11) Des-AA^{1,5}-[Tyr^2,D-Glu^7,D-Trp^8,IAmp^9,Dab^{11}]SRIF	19	93	96	1563.68	1564.5	>1K (2)	>1K (2)	>1K (2)	>1K (2)	>1K (2)
23	cyclo(7−11) Des-AA^{1,5}-[Tyr^2,Glu^7,D-Trp^8,IAmp^9,Lys^{11}]SRIF	21	98	98	1591.71	1592.7	>1K (2)	>1K (2)	>1K (2)	>1K (2)	>1K (2)
24	cyclo(7−11) Des-AA^{1,5}-[Tyr^2,D-Glu^7,D-Trp^8,IAmp^9,D-Dab^{11}]SRIF	19	94	91	1565.68	1566.7	>1K (2)	>1K (2)	>1K (2)	>1K (2)	>1K (2)
25	cyclo(7−12) Des-AA^{1,5}-[Tyr^2,Asp^7,D-Trp^8,IAmp^9,Dap^{12}]SRIF	20	97	>98	1583.67	1584.8	>1K (3)	>1K (2)	>1K (2)	>1K (2)	>1K (2)
26	cyclo(7−12) Des-AA^{1,5}-[Tyr^2,Asp^7,D-Trp^8,IAmp^9,Orn^{12}]SRIF	22	98	>98	1610.70	1611.7	>1K (2)	>1K (2)	>1K (2)	>1K (2)	>1K (2)
27	cyclo(7−12) Des-AA^{1,5}-[Tyr^2,Glu^7,D-Trp^8,IAmp^9,Dab^{12}]SRIF	22	>98	>98	1611.92	1612.8	241 ± 74 (4)	>1K (2)	>1K (2)	>1K (2)	>1K (2)
28	cyclo(7−12) Des-AA^{1,5}-[Tyr^2,Glu^7,D-Trp^8,IAmp^9,Orn^{12}]SRIF	23	>98	>98	1624.72	1625.7	554 (600, 508)	>1K (3)	>1K (3)	>1K (3)	>1K (3)
29	cyclo(7−12) Des-AA^{1,5}-[Tyr^2,Glu^7,D-Trp^8,IAmp^9,Lys^{12}]SRIF	24	95	96	1637.74	1638.7	53 ± 18 (3)	>1K (3)	>1K (3)	>1K (3)	>1K (3)
30	cyclo(7−12) Des-AA^{1,5}-[Tyr^2,Glu^7,D-Trp^8,IAmp^9,hLys^{12}]SRIF	25	93	96	1652.75	1653.8	94 ± 4 (3)	>1K (3)	>1K (3)	>1K (3)	>1K (3)
31	cyclo(7−12) Des-AA^{1,5}-[Tyr^2,Glu^7,D-Trp^8,IAmp^9,hhLys^{12}]SRIF	26	98	>98	1666.75	1667.8	16 ± 6 (4)	>1K (4)	>1K (4)	>1K (4)	>1K (4)
32	cyclo(7−12) Des-AA^{1,5}-[Tyr^2,Glu^7,D-Trp^8,IAmp^9,D-hLys^{12}]SRIF	25	87	98	1652.75	1653.8	782 (864, 700)	>1K (2)	>1K (2)	99 (109, 89)	>1K (2)
33	cyclo(7−12) Des-AA^{1,5}-[Tyr^2,Glu^7,D-Trp^8,IAmp^9,D-hhLys^{12}]SRIF	26	95	>98	1666.75	1667.8	204 (267, 140)	>1K (2)	772 (538, 1005)	>1K (2)	>1K (2)
34	cyclo(7−12) Des-AA^{1,5}-[Tyr^2,Glu^7,D-Trp^8,IAmp^9,Dab(Gly)^{12}]SRIF	25	95	>98	1667.73	1668.8	>1K (2)	>1K (2)	>1K (2)	>1K (2)	>1K (2)
35	cyclo(7−12) Des-AA^{1,5}-[Tyr^2,Glu^7,D-Trp^8,IAmp^9,Dab(βAla)^{12}]SRIF	26	99	>98	1681.74	1682.8	74 ± 22 (3)	>1K (3)	>1K (3)	>1K (3)	>1K (3)
36	cyclo(7−12) Des-AA^{1,5}-[Tyr^2,Glu^7,D-Trp^8,IAmp^9,Dab(Gaba)^{12}]SRIF	27	97	>98	1694.76	1695.9	61 (72, 49)	>1K (2)	>1K (2)	>1K (2)	>1K (2)
37	cyclo(7−12) Des-AA^{1,5}-[Tyr^2,Glu^7,D-Trp^8,IAmp^9,Orn(βAla)^{12}]SRIF	27	98	>98	1695.77	1696.7	64 ± 5 (3)	>1K (3)	>1K (3)	>1K (3)	>1K (3)
38	cyclo(7−12) Des-AA^{1,5}-[Tyr^2,Glu^7,D-Trp^8,IAmp^9,Orn(Gaba)^{12}]SRIF	28	95	98	1708.77	1709.7	167 (115, 218)	>1K (3)	>1K (3)	>1K (3)	>1K (3)
39	cyclo(7−12) Des-AA^{1,5}-[Tyr^2,Glu^7,D-Trp^8,IAmp^9,Lys(Gaba)^{12}]SRIF	29	>98	>98	1722.79	1723.7	274 (329, 219)	>1K (2)	>1K (2)	>1K (2)	>1K (2)
40	cyclo(7−12) Des-AA^{1,5}-[m-I-Tyr^2,Glu^7,D-Trp^8,IAmp^9,Lys^{12}]SRIF	24	97	>98	1765.63	1766.6	89 (87, 91)	>1K (2)	>1K (2	>1K (2	>1K (2
41	cyclo(7−12) Des-AA^{1,5}-[Tyr^2,Glu^7,D-Trp^8,IAmp^9,Lys^{12}]-CbmSRIF	24	70	92	1680.70	1681.7	181 (200, 162)	>1K (2)	>1K (2)	>1K (2)	>1K (2)
42	cyclo(7−12) Des-AA^{1,2,5}-[Glu^7,D-Trp^8,IAmp^9,Tyr^{11},Lys^{12}]SRIF	24	>98	>98	1491.67	1492.6	18 (20, 15)	>1K (2)	>1K (2)	>1K (2)	>1K (2)
43	cyclo(7−12) Des-AA^{1,2,5}-[Glu^7,D-Trp^8,(NMe)IAmp^9,Tyr^{11},Lys^{12}]SRIF	24	96	>98	1505.69	1506.7	62 (83, 41)	>1K (2)	>1K (2)	>1K (2)	>1K (2)
44	cyclo(7−12) Des-AA^{1,2,5}-[Glu^7,D-Trp^8,(NMe)IAmp^9,m-I-Tyr^{11},Lys^{12}]SRIF	24	90	>98	1631.59	1632.6	14 (18, 9.7)	> 1K (2)	254 (260, 247)	>1K (2)	>1K (2)
45	cyclo(7−12) Des-AA^{1,2,5}-[Glu^7,D-Trp^8,IAmp^9,m-I-Tyr^{11},hhLys^{12}]SRIF	26	98	98	1645.57	1646.5	6.1 ± 0.6 (3)	>1K (3)	>1K (3)	>1K (3)	>1K (3)
46	cyclo(7−12) Des-AA^{1,2,5}-[Glu^7,D-Trp^8,(NMe)IAmp^9,m-I-Tyr^{11},hhLys^{12}]SRIF	26	93	95	1659.60	1660.5	46 (43, 48)	>1K (2)	>1K (2)	611 (537, 685)	>1K (2)
47	cyclo(7−12) Des-AA^{1,2,5}-[Glu^7,D-Trp^8,IAmp^9,m-I-Tyr^{11},D-hhLys^{12}]SRIF	26	94	97	1645.57	1646.7	259 (252, 266)	>1K (2)	>1K (2)	>1K (2)	>1K (2)
48	cyclo(7−12) Des-AA^{1,2,5}-[Glu^7,D-Trp^8,(NMe)IAmp^9,m-I-Tyr^{11},D-hhLys^{12}]SRIF	26	70	80	1659.69	1660.6	620 (476, 763)	>1K (2)	>1K (2)	215 (190, 239)	>1K
49	cyclo(7−12) Des-AA$^{1-5,14}$-[Glu^7,D-Trp^8,IAmp^9,Lys^{12}]SRIF Phe-c[Glu-D-Trp-IAmp-Thr-Phe-Lys]-Ser-OH		98	97	1143.57	1144.6	>1K (2)	>1K (2)	>1K (2)	>1K (2)	>1K (2)

[a] Percent purity determined by HPLC using buffer system: A = TEAP (pH 2.5) and B = 60% CH_3CN/40% A with a gradient slope of 1% B/min, at flow rate of 0.2 mL/min on a Vydac C_{18} column (0.21 cm × 15 cm, 5-μm particle size, 300 Å pore size). Detection at 214 nm. [b] CZE was done using a Beckman P/ACE system 2050 controlled by an IBM Personal System/2 model 50Z and using a ChromJet integrator. Field strength of 15 kV at 30 °C, mobile phase: 100 mM sodium phosphate (85:15, H_2O/CH_3CN) pH 2.50, on a Supelco P175 capillary (363 μm o.d. × 75 μm i.d. × 50 cm length). Detection at 214 nm. [c] The calculated *m/z* of the monoisotope compared with the observed $[M+H]^+$ monoisotopic mass. [d] The IC_{50} values (nM) were derived from competitive radioligand displacement assays reflect the affinities of the analogues for the cloned somatostatin receptors using the nonselective ^{125}I-[Leu^8,D-Trp^{22},Tyr^{25}]SRIF-28, as the radioligand. Mean value ± SEM when $N \geq 3$ (shown in parentheses). Otherwise, mean with single values in parentheses. [e] Number of atoms in the cycle. [f] SRIF = H-Ala^1-Gly^2-c[Cys^3-Lys^4-Asn^5-Phe^6-Phe^7-Trp^8-Lys^9-Thr^{10}-Phe^{11}-Thr^{12}-Ser^{13}-Cys^{14}]-OH. [g] hLys = homo-lysine = 2,7-diaminoheptanoic acid; hhLys = homo-homo-lysine = 2,8-diaminooctanoic acid.

(CZE)) equivalent to that obtained nowadays using HPLC (Table 1).

Biological Testing. The compounds were tested for their ability to bind to 20 μm thick cryostat (Leitz 1720, Rockleigh, NJ) sections of a membrane pellet of cells transfected with each of the five human sst receptor subtypes as described earlier.[13,47−49] The most potent and selective analogues were then evaluated for their agonist/antagonist properties measuring the forskolin-stimulated production of cyclic adenosine monophosphate (cAMP).

Structure−Activity Relationships. After the observation that the N-terminus dipeptide of SRIF, the H-Ala-Gly-OH, could be deleted with retention of potencies in all of the assays available at the time (inhibition of GH, insulin, and glucagon),[50] most analogues of SRIF described in the literature are shortened at the N-terminus by two residues with the exception of those that have a tyrosine or a chelating agent for the purpose of labeling. Additionally, most somatostatin analogues have a D aromatic amino acid at position 8.[51] Here we show that deletion of one or several additional amino acids within the cycle of [D-Trp^8]SRIF results in either maintenance or loss of binding affinity at one or more receptors. Deletion of Lys^4 and Ser^{13} in addition to the N-terminus dipeptide yields **2**, which retains significant binding affinity except for sst$_1$. However, deletion of Lys^4-Asn^5 results in **3** with very high potency to inhibit GH and insulin while inactive at inhibiting glucagon secretion.[29−31,52]

Deletion of the additional Ser^{13} results in **4** with high binding affinity at sst$_2$ and sst$_4$, moderate binding affinity at sst$_3$ and sst$_5$, and poor binding affinity at sst$_1$. We have shown that introduction of IAmp^9 in the undecapeptide Des-AA^{1,2,5}-[D-Trp^8]SRIF to yield Des-AA^{1,2,5}-[D-Trp^8,IAmp^9]SRIF (CH-275) and in AA^{1,5}-[Tyr^2,D-Trp^8]SRIF to yield Des-AA^{1,5}-[Tyr^2,D-Trp^8,IAmp^9]-SRIF (CH-288, **14**) resulted in significant selectivity for sst$_1$ (IAmp = 4-(*N*-isopropyl)-aminomethylphenylalanine).[40] It was therefore hypothesized that the same substitution in an analogue shortened by two residues would retain such selectivity. The fact that **5** is essentially inactive at all of the receptors suggests that the scaffold of CH-275 is unique and necessary for both sst$_1$ affinity and selectivity. Deletion of one residue adjacent to Cys^3 and two residues adjacent to Cys^{14} to yield **6** favors sst$_4$ selectivity with retention of moderate binding affinity at all other receptors. Interestingly, deletion of Asn^5 rather than Lys^4 and the two residues adjacent to Cys^{14} yields **7** with increased binding affinity and similar sst$_4$ selectivity to that of **6**. This strongly suggests that a basic residue (in this case Lys^4 versus Asn^5) is important for receptor interaction. This finding is in keeping with the recent description of a biologically stable pan-somatostatin, KE108, where an arginine residue has been introduced at the equivalent position.[22] Substitution of Lys^9 by IAmp^9 in **7** to yield **8** abolishes binding affinity (>100-fold loss) at all of the receptors except possibly at sst$_1$. In Table 1, we also show the structure of ODT-8 (**9**) for reference purposes as this analogue has been extensively described in the literature and this scaffold was used for the discovery of sst$_3$-selective antagonists[53] and sst$_4$-selective agonists.[54] Further deletions as shown in **10**−**13** result in almost complete loss of binding affinity at each receptor and extremely low relative potencies to inhibit GH, insulin, and glucagon secretion.

When we compare binding affinities and relative potencies to inhibit GH, insulin, and glucagon, we find some correlation between sst$_2$ binding affinities and GH secretion as expected.[55,56] Although several of these shortened analogues (**2**−**4**, **6**, **7**, and **9**) are highly potent, there is no obvious correlation between their binding affinities and inhibition of GH, insulin, or glucagon. We suspect that the paucity of in vivo data and the fact that pituitary and pancreatic secretions may respond to the combined stimulation of more than one receptor, thus emphasizing the need for truly sst-selective ligands.

Because this first screen did not seem to identify promising leads for the design of constrained sst$_1$-selective analogues, we hypothesized that structural constraints such as internal lactam bridges in the lead sst$_1$-selective analogue (**14**, CH-288) could fulfill this aim.

An obvious bridging opportunity was suggested by the prior observation that stacking of benzene rings of the two phenylalanines at positions 6 and 11 played a significant role in stabilizing the structure of SRIF.[32,33] To prove this hypothesis, Veber et al. introduced covalent constraints between the side chains of residues at both positions 6 and 11, which resulted in analogues with retention of high potency in assays that measured inhibition of GH, insulin, and glucagon secretions. As shown in Table 2, using the radioiodinatable sst$_1$-selective CH-288 as a parent analogue, introduction of lactam rings of different sizes (22 atoms in **15** and 24 atoms in **17**) and configuration (D configuration at residues 6 and 11 in **16**) resulted in analogues that were essentially inactive. This suggested to us that either or both phenylalanines were critical elements of a putative sst$_1$ pharmacophore. Alternatively, such bridging prevented the analogues from assuming an sst$_1$-compatible conformation. Whereas an Asp^6-Dap^{12} lactam bridge in CH-288 led to the inactive **18** (23 atoms in the cycle), the less constrained Glu^6-Dab^{12} lactam bridge (25 atoms in the cycle) led to **19** with both limited binding affinity (IC$_{50}$ = 104 nM) and sst$_1$-selectivity (>10-fold) (Dap = 2,3-diaminopropionic acid, Dab = 2,4-diaminobutyric acid). The fact that a larger ring size (27 atoms as in **20**) led to a less potent analogue suggested that the extension of the ring size had reached its optimal length (25 atoms) and configuration as shown in **19**. We then moved the head of the bridge to position 7 and found that none of the analogues with bridges from Xaa^7 to Xbb^{11} (**21**−**23**, with ring sizes ranging from 19 to 21 atoms) or D-Glu^7 to D-Dab^{11} (**24**) had any affinity for any of the five sst.

However, first attempts at bridging side chains at positions 7 and 12 seemed more promising. Systematically increasing the size of the bridging ring going from 20-atom-membered rings (**25**) to 26-atom-membered rings (**26**−**30**) ultimately led to **31** with a binding affinity comparable to that of the parent CH-288. It is noteworthy that two analogues (**26** and **27**) with the same number of atoms in the cycle yet with the lactam bridge shifted by one methylene group (Asp^7 to Orn^{12} in **26** versus Glu^7 to Dab^{12} in **27**) differ in their binding affinities for sst$_1$; **27** shows at least 5 times greater

binding affinity at sst_1 than **26**. This emphasizes how important it is to mimic as closely as possible the bioactive conformation and placement of functional groups found in the native molecule in order to elicit high binding.

We then synthesized a series of analogues in which the length of the side chain at position 12 was incrementally increased by one methylene group (**27**−**31**) while retaining Glu at position 7. A 5-fold increase in sst_1-binding affinity was observed when the ring size was increased from 22 (**27**) to 24 (**29**) atoms and by as much as 15 times when the number of atoms in the cycle is increased from 22 (**27**) to 26 (**31**) atoms using Dab^{12} (**27**, IC_{50} = 241 nM at sst_1), Orn^{12} (**28**, IC_{50} = 554 nM at sst_1), Lys^{12} (**29**, IC_{50} = 53 nM at sst_1), $hLys^{12}$ (**30**, IC_{50} = 94 nM at sst_1), and $hhLys^{12}$ (**31**, IC_{50} = 16 nM at sst_1), respectively. We have no explanation why the overall improvement in binding affinity with increasing size of the lactam bridge is not linear as **28** and **30** have sst_1-binding affinities somewhat worse than expected. Noteworthy is that **31**, dicyclo (3−14, 7−12)H-Tyr^2-Cys^3-Lys^4-Phe^6-Glu^7-D-Trp^8-$IAmp^9$-Thr^{10}-Phe^{11}-$hhLys^{12}$-Ser^{13}-Cys^{14}-OH (i.e., cyclo(7−12) Des-$AA^{1,5}$-[Tyr^2,Glu^7, D-Trp^8,$IAmp^9$,$hhLys^{12}$]SRIF) has a binding affinity comparable to that of its parent **14**. Because we used D,L-hLys and D,L-hhLys in the synthesis of **30** and **31**, we were able to also isolate in highly purified form the diastereomers **32** (IC_{50} = 782 nM at sst_1) and **33** (IC_{50} = 204 nM at sst_1) (hLys = homo-lysine = 2,7-diaminoheptanoic acid, hhLys = homo-homo-lysine = 2,8-diaminooctanoic acid). We cannot exclude the possibility that some of the binding affinity of these analogues is due to some minor contamination by the parent **30** and **31**. It is however clear that a D residue at position 12 is detrimental to binding affinity.

Another strategy to increase the size of a bridge is to include an additional amino acid such as Gly (**34**), βAla (**35**), and Gaba (**36**) in the cycle (Gaba = γ-aminobutyric acid). Whereas **34** with 25 atoms in the cycle was inactive at all receptors, **35** (26 atoms in the ring) and **36** (27 atoms in the ring) were comparable in size to **31** and were equipotent (IC_{50} = 74 and 61 nM at sst_1, for **35** and **36**, respectively) and selective (>10-fold) for sst_1. Following the same strategy of further increasing the size of the lactam bridge using an additional amino acid, we synthesized **37**−**39** (27 to 29 atoms in the cycle, respectively), which showed mediocre affinity and sst_1-selectivity.

One advantage of developing subtype-selective analogues is to be able to radiolabel them and use them as in vitro tracers to selectively detect sst_1 tissues or, as in vivo tracers, for diagnostic purposes or for tumor treatment. Within these premises, we synthesized the monoiodinated **40**, which resulted in an IC_{50} = 89 nM at sst_1 comparable to that of its parent **29** which is clearly inadequate for diagnostic or therapeutic purposes. Carbamoylation of the N-terminus has been shown earlier to be a favorable substitution in the design of sst_1-selective analogues.[57] This substitution, introduced in **29** to yield **41**, is clearly unfavorable because it resulted in a 4-fold increase in IC_{50}. Previous results showing that the introduction of a tyrosine at other positions than position 2 could have a beneficial effect on potency led us to synthesize **42** with a tyrosine

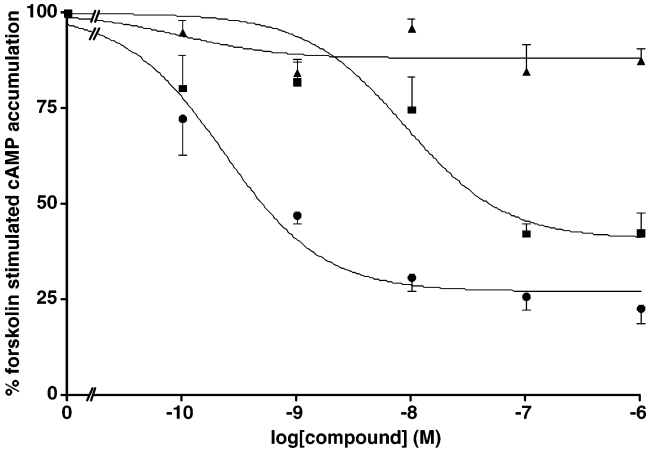

Figure 2. Effect of various concentrations of the sst_1-selective agonist (**45**) and the sst_3-selective antagonist sst_3−ODN-8,[53] in comparison with SRIF-28 as positive control, on forskolin-stimulated cAMP accumulation in CCL39 cells expressing sst_1. Concentration−response curves were obtained with increasing concentrations of SRIF-28 (●) (EC_{50} = 0.23 nM) and **45** (■) (EC_{50} = 8.8 nM). Sst_3-ODN-8 (▲), as negative control, has no effect. Data are expressed as % forskolin-stimulated cAMP accumulation. The plot represents the mean of four independent experiments in triplicate (mean ± SEM).

residue at position 11. The IC_{50} value of **42** (18 nM at sst_1) is about 3 times lower than that of the homologous **29** (53 nM at sst_1). We then wondered whether an additional constraint-inducing modification such as N^{α}-methylation of residue 9 shown earlier to be favorable[13] would further enhance sst_1-biding affinity. An IC_{50} = 62 nM at sst_1 for **43** suggested otherwise. Monoiodination of **43**, yielding **44**, however, resurrected high-binding affinity as shown earlier in some instances.[57] From these data, we concluded that N^{α}-methylation of residue 9 in dicyclic analogues was not favorable in contradistinction with monoiodination of Tyr^{11}. Hence, we synthesized **45**, related to **31**, our best analogue so far, with an hhLys residue at position 12. This combination of substitutions m-I-Tyr^{11},$hhLys^{12}$ in the Des-$AA^{1,2,5}$-cyclo(7−12) [Glu^7,D-Trp^8,$IAmp^9$]SRIF scaffold is clearly optimized as it resulted in **45** with an IC_{50} = 6.1 nM at sst_1. N^{α}-Methylation of **45** at position 9 to yield **46** was clearly detrimental. As in the case of **32** and **33**, the D-hhLys-containing isomers (**47**, **48**) of **45** and **46** were significantly less potent.

Finally, to test our earlier premises that once we had identified a dicyclic analogue with high affinity we could likely eliminate the cystine-containing ring as superfluous, we synthesized cyclo(7−12) Des-$AA^{1-5,14}$-[Glu^7,D-Trp^8,$IAmp^9$,Lys^{12}]SRIF (i.e., H-Phe^6-cyclo[Glu^7-D-Trp^8-$IAmp^9$-Thr^{10}-Phe^{11}-Lys^{12}]-Ser^{13}-OH) (**49**) the supposedly active core of the sst_1 pharmacophore. This is in keeping with the observation of Veber et al. that the potent dicyclic SRIF analogue cyclo[Lys-Cys-Phe-Phe-D-Trp-Lys-Thr-Phe-Cys-Ser][32,33] could be shortened to yield the already known ODT-8 (Figure 1B)[18,19] upon deletion of the Ser-Lys residues forming the second ring. The octapeptide **49** is inactive at all receptors suggesting that the constraint resulting from the presence of the second cycle or the functional groups present in that cycle are important for receptor recognition and activation.

To distinguish agonists from antagonists, the effect of our best sst_1 analogue (**45**) was evaluated on forsko-

lin-stimulated cAMP production in sst_1-expressing CCL39 cells. The data are shown in Figure 2. The agonist somostatin-28 (SRIF-28) potently inhibited forskolin-stimulated cAMP accumulation by more than 74% at a peptide concentration of 100 nM, with an $EC_{50} = 0.23$ nM; it was used as positive control. Our best sst_1 analogue (**45**) was tested in this system and showed agonistic properties with an $EC_{50} = 8.8$ nM. The sst_3-selective sst_3−ODN-8[53] was used as negative control. In addition, we tested compound **45** in the presence of an increasing dose of SRIF-28 in order to further exclude antagonistic properties of **45**. The agonistic effect of SRIF-28 seen in concentration−response curves could indeed not be antagonized with a fixed concentration of 200 nM of **45**, confirming the agonistic properties of **45** (data not shown).

Conclusions

Using an iterative approach to the design of high affinity sst_1-selective analogues with constrained structures, we identified dicyclo(3−14, 7−12)H-Cys[3]-Lys[4]-Phe[6]-Glu[7]-D-Trp[8]-IAmp[9]-Thr[10]-m-I-Tyr[11]-hhLys[12]-Ser[13]-Cys[14]-OH (**45**) as the most potent and sst_1-selective analogue reported so far. Because structural constraints may interfere with receptor activation, it was imperative to demonstrate that **45** was an agonist. Interestingly, the additional constraint {cyclo(7−12)} that led to retention of sst_1-selectivity is different from that identified by Veber et al. that yielded mostly sst_2 selectivity. Unlike Veber's discovery that the cycle furthest from the turn defined by Phe-Trp-Lys-Thr could be deleted, our shortened analogues lost binding affinity, suggesting an important role for the amino acids at positions 4, 6, and 13 as shown in the proposed consensus NMR-derived bioactive conformation described in the following paper.[12]

Experimental Procedures

Starting Materials. The Boc-Cys(Mob)-CM resin with a capacity of 0.3−0.5 mequiv/g was obtained according to published procedures (Mob = 4-methoxybenzyl).[58] All of the N^{α}-*tert*-butoxycarbonyl (BOC) protected amino acids with side chain protection were purchased from Bachem Inc. (Torrance, CA), Chem-Impex Intl. (Wood Dale, IL), Novabiochem (San Diego, CA), or Reanal (Budapest, Hungary). The side chain protecting groups were as follows: Asp(OFm), Cys(Mob), Dab(Fmoc), Dap(Fmoc), Glu(OFm), Lys[Z(2Cl)], Lys(Fmoc), Orn(Fmoc), Ser(Bzl), Thr(Bzl), Tyr[Z(2Br)], m-I-Tyr[Bzl(3Br)]. Boc-IAmp(Z),[59] Boc-D/L-hLys(Fmoc), and Boc-D/L-hhLys(Fmoc)[60] were synthesized in our laboratory (Z = benzyloxycarbonyl, Bzl = benzyl, Bzl(3Br) = 3-bromobenzyl, Z(2Br) = 2-bromobenzyloxycarbonyl, Z(2Cl) = 2-chlorobenzyloxycarbonyl. Fmoc-β-Ala and Fmoc-Gaba were the products of Chem-Impex Intl. (Wood Dale, IL). Boc-N^{α}Me-IAmp(Z) was also synthesized in our laboratory as described in the literature.[13,61] Trypsin was purchased from Roche Molecular Biochemicals (U.S.A.). All of the reagents and solvents were reagent grade or better and used without further purification.

Peptide Synthesis. Peptides were synthesized by the solid-phase approach with Boc chemistry either manually or on a CS-Bio Peptide Synthesizer model CS536. Boc-Cys(Mob)-CM resin with a capacity of 0.3−0.5 mequiv/g was used. Couplings of the protected amino acids were mediated by DIC in CH_2Cl_2 or *N*-methylpyrrolidinone (NMP) for 1 h and monitored by the qualitative ninhydrin test.[62] A 3-equiv excess of the protected amino acids based on the original substitution of the resin was used in most cases. Boc removal was achieved with trifluoroacetic acid (60% in CH_2Cl_2, 1−2% *m*-cresol) for 20 min. An isopropyl alcohol (1% *m*-cresol) wash followed trifluoroacetic acid (TFA) treatment and then successive washes with triethylamine solution (10% in CH_2Cl_2), methanol, triethylamine solution, methanol, and CH_2Cl_2 completed the neutralization sequence. After complete synthesis of peptide sequence, lactam bridges were constructed on the resin by first treating the orthogonally protected peptide with 20% piperidine in NMP in two successive 5 and 15 min treatments to remove the Fmoc and OFm protecting groups from the side chain of Dab, Dap, Lys, hLys, hhLys, Orn, Asp, and Glu, followed by the addition of 2 equiv of TBTU in NMP while solution was kept basic by the addition of *N*,*N*-diisopropylethylamine (DIPEA). In **34**−**39,** at position 12, Fmoc-β-Ala and Fmoc-Gaba were coupled to the deprotected side chains of Dab, Dbu, Lys, and Orn, on the resin before the synthesis proceeded to the coupling of the amino acid at position 11. The ureido group (Cbm = carbamoyl) at the N-terminus of **41** was introduced on the resin.[13] The monocyclic and fully protected peptide was finally cleaved from the resin support with simultaneous side chain deprotection by anhydrous HF containing the scavengers anisole (10% v/v) and methyl sulfide (5% v/v) for 60 min at 0 °C. The diethyl ether precipitated crude peptides were cyclized in 75% acetic acid (200 mL) by addition of iodine (10% solution in methanol) until the appearance of a stable orange color. Forty minutes later, ascorbic acid was added to quench the excess of iodine.

Determination of the Chirality of hLys and hhLys in Peptides 30 and 32 and 31, 33, and 45−48. First, the hLys and hhLys-containing peptides (**30** and **32** and **31**, **33**, and **45**−**48**, respectively) were synthesized using unresolved Boc-D/L-hLys(Fmoc) and Boc-D/L-hhLys(Fmoc), respectively. The diastereomers **30/32**, **31/33**, **45/47**, and **46/48** were separated by preparative RP-HPLC. The absolute configuration of hLys and hhLys in the analogues was deduced from enzymatic hydrolysis studies with trypsin. Trypsin (5 μg in 0.05% TFA, 20 μL) was added to the peptides (20 μg) dissolved in 0.046 M TRIS buffer containing 0.01 M $CaCl_2$, pH 8.1 (80 μL) at room temperature. The hydrolysis of the peptides was monitored by RP-HPLC. When it was possible, the mass of the resulting fragments was determined by MALDI mass spectrometry. The observed masses were matched up to the calculated masses for the predicted degradation products. A 12-day digestion of **30** resulted in several products. The major product had a mass of 1071.68. This mass could be matched to that of cyclo(7−12)H-Phe[6]-Glu[7]-D-Trp[8]-IAmp[9]-Thr[10]-Phe[11]-hLys[12]-OH (SRIF numbering). The digestion of **32** resulted in a major product that showed a higher mass by 18 indicating only a ring opening and among the several minor products, the smallest observed mass was 1261.51. This mass could be assigned to that of cyclo-(7−12)H-Phe[6]-Glu[7]-D-Trp[8]-IAmp[9]-Thr[10]-Phe[11]-hLys[12]-Ser[13]-Cys[14]-OH, suggesting that **30** contains the L isomer of the hLys and **32** contains the D isomer of hLys. The exact same patterns were found for **31/33**, **45/47**, and **46/48**. A mass of 1107.52 Da, which could be matched to that of cyclo(7−12)H-Phe[6]-Glu[7]-D-Trp[8]-IAmp[9]-Thr[10]-Phe[11]-hhLys[12]-OH, and a mass 1275.73, which could be matched to that of cyclo(7−12)H-Phe[6]-Glu[7]-D-Trp[8]-IAmp[9]-Thr[10]-Phe[11]-hhLys[12]-Ser[13]-Cys[14]-OH, were observed. These findings suggest that **31**, **45**, and **46** have the L-hhLys in the sequence and **33**, **47**, and **48** contain the D-hhLys in the sequence.

Purification and Characterization. The crude, lyophilized peptides were purified by preparative RP-HPLC[45] on a 5 cm × 30 cm cartridge, packed in the laboratory with reversed-phase 300-Å Vydac C_{18} silica (15−20 μm particle size) using a Waters Associates (Milford, MA) DeltaPrep 3000 system, model Shimadzu SPD-6A variable wavelength UV detector, and Huston Instruments Omni Scribe chart recorder. The peptides eluted with a flow rate of 100 mL/min using a linear gradient of 1% B per 3 min increase from the baseline %B. (Eluent A = 0.25 N TEAP pH 2.25; eluent B = 60% CH_3CN, 40% A) (TEAP = triethylammonium phosphate). As a final step, all of the peptides were rechromatographed in a 0.1% TFA solution and acetonitrile on the same cartridge at 100 mL/min (gradient of 1% acetonitrile/min). Analytical RP-HPLC screening was performed on a Vydac C_{18} column (0.46

cm × 25 cm, 5-μm particle size, 300-Å pore size) connected to a Rheodyne model 7125 injector, an Altex 420 HPLC system using two Altex 100A pumps, a Kratos Spectroflow 757 UV detector set to 210 nm, and a Houston Instruments D-5000 strip chart recorder. The fractions containing the product were pooled and subjected to lyophilization. The diastereomer analogues **30/32**, **31/33, 45/47**, and **46/48** were separated by preparative RP-HPLC. The purity of the final peptides was determined by analytical RP-HPLC performed with a linear gradient using 0.1 M TEAP pH 2.5 as eluent A and 60% CH_3CN/40% A as eluent B on a Hewlett-Packard series II 1090 liquid chromatograph connected to a Vydac C_{18} column (0.21 cm × 15 cm, 5-μm particle size, 300-Å pore size), Controller model 362, and a Think Jet printer. CZE analysis was performed on a Beckman P/ACE system 2050 controlled by an IBM Personal System/2 model 50Z connected to a ChromJet integrator.[46] Complete details are shown in Tables 1 and 2. Mass spectra (MALDI-TOF MS) were measured on an ABI-Perseptive DE-STR instrument. The instrument employs a nitrogen laser (337 nm) at a repetition rate of 20 Hz. The applied accelerating voltage was 20 kV. Spectra were recorded in delayed extraction mode (300 ns delay). All of the spectra were recorded in the positive reflector mode. Spectra were sums of 100 laser shots. Matrix α-cyano-4-hydroxycinnamic acid was prepared as saturated solutions in 0.3% trifluoroacetic acid in 50% acetonitrile. The observed monoisotopic $(M + H)^+$ values of each peptide corresponded with the calculated (*M*) values (Tables 1 and 2).

Receptor Autoradiography. Cells stably expressing the cloned five human sst (CHO-K1 for sst_1 and sst_5 and CCL39 for sst_2, sst_3, and sst_4) were grown as previously described.[47] All of the cell culture reagents were supplied by Gibco BRL, Life Technologies (Grand Island, NY). The receptor autoradiographical experiments were performed as reported previously,[47] using ^{125}I-Tyr-[Leu^8,D-Trp^{22},Tyr^{25}]SRIF-28 as tracer.

Adenylate Cyclase Activity. Modulation of forskolin-stimulated adenylate cyclase activity was determined using a radioimmunoassay measuring intracellular cAMP levels by competition binding[22] as described in part 2 for sst_1-expressing CCL39 cells.[13]

Acknowledgment. This work was supported in part by NIH Grant RO1 DK 59953 (U.S.A.). We are indebted to W. Low, R. Kaiser, and C. Miller for technical assistance in the synthesis and characterization of the peptides, to Dr. W. Fisher for mass spectrometric analysis of the analogues, and to D. Doan for manuscript preparation. CHO-K1 cells stably expressing human sst_1 and sst_5 were kindly provided by Drs. T. Reisine and G. Singh (University of Pennsylvania, Philadelphia, PA), and CCL39 cells stably expressing human sst_1, sst_2, sst_3, and sst_4 by Dr. D. Hoyer (Novartis Pharma, Basel, Switzerland). J.R. is the Dr. Frederik Paulsen Chair in Neurosciences Professor.

References

(1) Burgus, R.; Brazeau, P.; Vale, W. W. Isolation and determination of the primary structure of somatostatin (a somatotropin release inhibiting factor) of ovine hypothalamic origin. *Advances in Human Growth Hormone Research*; U.S. Government Printing Office, DHEW, Publ No. (NIH) 74-612, 1973; pp 144−158.
(2) Brazeau, P.; Vale, W. W.; Burgus, R.; Ling, N.; Butcher, M. et al. Hypothalamic polypeptide that inhibits the secretion of immunoreactive pituitary growth hormone. *Science* **1973**, *179*, 77−79.
(3) Rivier, J. Somatostatin: Total solid-phase synthesis. *J. Am. Chem. Soc.* **1974**, *96*, 2986−2992.
(4) Meyerhof, W.; Paust, H. J.; Schoenrock, C.; Richter, D. Cloning of a cDNA encoding a novel putative G-protein-coupled receptor expressed in specific rat brain regions. *DNA Cell Biol.* **1991**, *10*, 689−694.
(5) Meyerhof, W.; Wulfsen, I.; Schönrock, C.; Fehr, S.; Richter, D. Molecular cloning of a somatostatin-28 receptor and comparison of its expression pattern with that of a somatostatin-14 receptor in rat brain. *Proc. Natl. Acad. Sci. U.S.A.* **1992**, *89*, 10267−10271.
(6) Bruno, J. F.; Xu, Y.; Song, J.; Berelowitz, M. Molecular cloning and functional expression of a brain-specific somatostatin receptor. *Proc. Natl. Acad. Sci. U.S.A.* **1992**, *89*, 11151−11155.
(7) Rohrer, L.; Raulf, F.; Bruns, C.; Buettner, R.; Hofstaedter, F. et al. Cloning and characterization of a fourth human somatostatin receptor. *Proc. Natl. Acad. Sci. U.S.A.* **1993**, *90*, 4196−4200.
(8) Xu, Y.; Song, H.; Bruno, J. F.; Berelowitz, M. Molecular cloning and sequencing of a human somatostatin receptor, hSSTR4. *Biochem. Biophys. Res. Commun.* **1993**, *193*, 648−652.
(9) Yamada, Y.; Post, S. R.; Wang, K.; Medical, H.; Tager, S. et al. Cloning and functional characterization of a family of human and mouse somatostatin receptors expressed in brain, gastrointestinal tract, and kidney. *Proc. Natl. Acad. Sci. U.S.A.* **1992**, *89*, 251−255.
(10) Yamada, Y.; Kagimoto, S.; Kubota, A.; Yasuda, K.; Masuda, K. et al. Cloning, functional expression and pharmacological characterization of a fourth (hSSTR4) and fifth (hSSTR5) human somatostatin receptor subtype. *Biochem. Biophys. Res. Commun.* **1993**, *195*, 844−852.
(11) Koerker, D. J.; Ruch, W.; Chideckel, E.; Palmer, J.; Goodner, C. J. et al. Somatostatin: hypothalamic inhibitor of the endocrine pancreas. *Science* **1974**, *184*, 482−484.
(12) Grace, C. R. R.; Durrer, L.; Koerber, S. C.; Erchegyi, J.; Reubi, J. C. et al. Somatostatin receptor 1 selective analogues: 4. Three-dimensional consensus structure by NMR. *J. Med. Chem.* **2005**, *48*, 523−533.
(13) Erchegyi, J.; Hoeger, C.; Low, W.; Hoyer, D.; Waser, B. et al. Somatostatin receptor 1 selective analogues: 2. N$^\alpha$-methylated scan. *J. Med. Chem.* **2005**, *48*, 507−514.
(14) Janecka, A.; Zubrzycka, M.; Janecki, T. Review: Somatostatin analogs. *J. Pept. Res.* **2001**, *58*, 91−107.
(15) Woltering, E. A. Development of targeted somatostatin-based antiangiogenic therapy: A review and future perspectives. *Cancer Biother. Radiopharm.* **2003**, *18*, 601−609.
(16) Froidevaux, S.; Eberle, A. N. Somatostatin analogs and radiopeptides in cancer therapy. *Biopolymers* **2002**, *66*, 161−183.
(17) Reubi, J. C. Peptide receptors as molecular targets for cancer diagnosis and therapy. *Endocr. Rev.* **2003**, *24*, 389−427.
(18) Vale, W.; Rivier, C.; Brown, M.; Rivier, J. Pharmacology of TRF, LRF and somatostatin. *Hypothalamic Peptide Hormones and Pituitary Regulation: Advances in Experimental Medicine and Biology*; Plenum Press: New York, 1977; pp 123−156.
(19) Vale, W.; Rivier, J.; Ling, N.; Brown, M. Biologic and immunologic activities and applications of somatostatin analogs. *Metabolism* **1978**, *27*, 1391−1401.
(20) Bauer, W.; Briner, U.; Doepfner, W.; Haller, R.; Huguenin, R.; et al. SMS 201−995: a very potent and selective octapeptide analog of somatostatin with prolonged action. *Life Sci.* **1982**, *31*, 1133−1140.
(21) Weckbecker, G.; Briner, U.; Lewis, I.; Bruns, C. SOM230: A new somatostatin peptidomimetic with potent inhibitory effects on the growth hormone/insulin-like growth factor-I axis in rats, primates, and dogs. *Endocrinology* **2002**, *143*, 4123−4130.
(22) Reubi, J. C.; Eisenwiener, K. P.; Rink, H.; Waser, B.; Macke, H. R. A new peptidic somatostatin agonist with high affinity to all five somatostatin receptors. *Eur. J. Pharmacol.* **2002**, *456*, 45−49.
(23) Sassolas, G. The role of Sandostatin in acromegaly. *Metab., Clin. Exp.* **1992**, *41*, 39−43.
(24) Grosman, I.; Simon, D. Potential gastrointestinal uses of somatostain and its synthetic analogue octreotide. (Review). *Am. J. Gastroenterol.* **1990**, *85*, 1061−1072.
(25) Lamberts, S. W.; van der Lely, A. J.; Hofland, L. J. New somatostatin analogs: will they fulfill old promises? *Eur. J. Endocrinol.* **2002**, *146*, 701−705.
(26) Ösapay, G.; Ösapay, K. Therapeutic applications of somatostatin analogues. *Expert Opin. Ther. Patents* **1998**, *8*, 855−870.
(27) Weckbecker, G.; Lewis, I.; Albert, R.; Schmid, H. A.; Hoyer, D. et al. Opportunities in somatostatin research: biological, chemical and therapeutic aspects. *Nat. Rev. Drug Discov.* **2003**, *2*, 999−1017.
(28) Brown, M.; Rivier, J.; Vale, W. W. Biological activity of somatostatin and somatostatin analogs on inhibition of arginine-induced insulin and glucagon release in rat. *Endocrinology* **1976**, *98*, 336−343.
(29) Brown, M.; Rivier, J.; Vale, W. W. Somatostatin analogs wih selected biologic activities. *Metabolism* **1976**, *25*, 1501−1503.
(30) Brown, M.; Rivier, J.; Vale, W. W. Somatostatin: analogs with selected biological activities. *Science* **1977**, *196*, 1467−1468.
(31) Brown, M.; Rivier, J.; Vale, W. W. Somatostatin central nervous system (CNS) action on glucoregulation. *Metabolism* **1978**, *27*, 1253−1256.

(32) Veber, D. F.; Holly, F. W.; Paleveda, W. J.; Nutt, R. F.; Bergstrand, S. J. et al. Conformationally restricted bicyclic analogs of somatostatin. *Proc. Natl. Acad. Sci. U.S.A.* **1978**, *75*, 2636−2640.
(33) Veber, D. F.; Holly, F. W.; Nutt, R. F.; Bergstrand, S. J.; Brady, S. F. et al. Highly active cyclic and bicyclic somatostatin analogues of reduced ring size. *Nature* **1979**, *280*, 512−514.
(34) Veber, D. F.; Freidinger, R. M.; Perlow, D. S.; Paleveda, W. J., Jr.; Holly, F. W. et al. A potent cyclic hexapeptide analogue of somatostatin. *Nature* **1981**, *292*, 55−58.
(35) Falb, E.; Salitra, Y.; Yechezkel, T.; Bracha, M.; Litman, P. et al. A bicyclic and hsst2 selective somatostatin analogue: design, synthesis, conformational analysis and binding. *Bioorg. Med. Chem.* **2001**, *9*, 3255−3264.
(36) Jiang, S.; Gazal, S.; Gelerman, G.; Ziv, O.; Karpov, O. et al. A bioactive somatostatin analog without a type II′ beta-turn: synthesis and conformational analysis in solution. *J. Pept. Sci.* **2001**, *7*, 521−528.
(37) Mattern, R.-H.; Zhang, L.; Rueter, J. K.; Goodman, M. Conformational analyses of sandostatin analogs containing stereochemical changes in positions 6 or 8. *Biopolymers* **2000**, *53*, 506−522.
(38) Mattern, R. H.; Tran, T. A.; Goodman, M. Conformational analyses of cyclic hexapeptide analogs of somatostatin containing arylalkyl peptoid and naphthylalanine residues. *J. Pept. Sci.* **1999**, *5*, 161−175.
(39) Grace, C. R. R.; Erchegyi, J.; Koerber, S. C.; Reubi, J. C.; Rivier, J. et al. Novel sst_4-selective somatostatin (SRIF) agonists. Part IV: Three-dimensional consensus structure by NMR. *J. Med. Chem.* **2003**, *46*, 5606−5618.
(40) Liapakis, G.; Hoeger, C.; Rivier, J.; Reisine, T. Development of a selective agonist at the somatostatin receptor subtype SSTR1. *J. Pharmacol. Exp. Ther.* **1996**, *276*, 1089−1094.
(41) Sarantakis, D.; McKinley, W. A.; Jaunakais, I.; Clark, D.; Grant, N. H. Structure activity studies on somatostatin. *Clin. Endocrinol.* **1976**, *5*, 275s-278s.
(42) Veber, D. F. Design and discovery in the development of peptide analogs. *Twelfth American Peptide Symposium*; Peptides: Chemistry and Biology: Cambridge, MA, June 16−21, 1991; pp 1−14.
(43) Felix, A. M.; Wang, C.-T.; Campbell, R. M.; Toome, V.; Fry, D. C. et al. Biologically active cyclic (lactam) analogs of growth hormone-releasing factor: Effect of ring size and location on conformation and biological activity. *Twelfth American Peptide Symposium*; Peptides, Chemistry and Biology: Cambridge, MA, June 16−21, 1991; pp 77−79.
(44) Erchegyi, J.; Penke, B.; Simon, L.; Michaelson, S.; Wenger, S. et al. Novel sst_4-selective somatostatin (SRIF) agonists. Part II: Analogues with β-methyl-3-(2-naphthyl)-alanine substitutions at position 8. *J. Med. Chem.* **2003**, *46*, 5587−5596.
(45) Miller, C.; Rivier, J. Peptide chemistry: Development of high-performance liquid chromatography and capillary zone electrophoresis. *Biopolymers* **1996**, *40*, 265−317.
(46) Miller, C.; Rivier, J. Analysis of synthetic peptides by capillary zone electrophoresis in organic/aqueous buffers. *J. Pept. Res.* **1998**, *51*, 444−451.
(47) Reubi, J. C.; Schaer, J. C.; Waser, B.; Wenger, S.; Heppeler, A. et al. Affinity profiles for human somatostatin receptor sst1-sst5 of somatostatin radiotracers selected for scintigraphic and radiotherapeutic use. *Eur. J. Nucl. Med.* **2000**, *27*, 273−282.
(48) Reubi, J. C.; Schaer, J. C.; Waser, B.; Hoeger, C.; Rivier, J. A selective analog for the somatostatin sst1-receptor subtype expressed by human tumors. *Eur. J. Pharmacol.* **1998**, *345*, 103−110.
(49) Reubi, J. C. In vitro identification of vasoactive intestinal peptide receptors in human tumors: Implications for tumor imaging. *J. Nucl. Med.* **1995**, *36*, 1846−1853.
(50) Rivier, J.; Brazeau, P.; Vale, W.; Guillemin, R. Somatostatin analogs: Relative importance of the disulfide bridge and of the Ala-Gly side chain for biological activity. *J. Med. Chem.* **1975**, *18*, 123−126.
(51) Rivier, J.; Brown, M.; Vale, W. [D-Trp8]-somatostatin: An analog of somatostatin more potent than the native molecule. *Biochem. Biophys. Res. Commun.* **1975**, *65*, 746−751.
(52) Brown, M. R.; Rivier, J.; Vale, W. W. Somatostatin: Central nervous system actions on glucoregulation. *Endocrinology* **1979**, *104*, 1709−1715.
(53) Reubi, J. C.; Schaer, J.-C.; Wenger, S.; Hoeger, C.; Erchegyi, J. et al. SST3-selective potent peptidic somatostatin receptor antagonists. *Proc. Natl. Acad. Sci. U.S.A.* **2000**, *97*, 13973−13978.
(54) Rivier, J.; Erchegyi, J.; Hoeger, C.; Miller, C.; Low, W. et al. Novel sst_4-selective somatostatin (SRIF) agonists. Part I: Lead identification using a betide scan. *J. Med. Chem.* **2003**, *46*, 5579−5586.
(55) Parmar, R. M.; Chan, W. W.-S.; Dashkevicz, M.; Hayes, E. C.; Rohrer, S. P. et al. Nonpeptidyl somatostatin agonists demonstrate that sst2 and sst5 inhibit stimulated growth hormone secretion from rat anterior pituitary cells. *Biochem. Biophys. Res. Commun.* **1999**, *263*, 276−280.
(56) Tulipano, G.; Soldi, D.; Bagnasco, M.; Culler, M. D.; Taylor, J. E. et al. Characterization of new selective somatostatin receptor subtype-2 (sst2) antagonists, BIM-23627 and BIM-23454. Effects of BIM-23627 on GH release in anesthetized male rats after short-term high-dose dexamethasone treatment. *Endocrinology* **2002**, *143*, 1218−1224.
(57) Rivier, J. E.; Hoeger, C.; Erchegyi, J.; Gulyas, J.; DeBoard, R. et al. Potent somatostatin undecapeptide agonists selective for somatostatin receptor 1 (sst1). *J. Med. Chem.* **2001**, *44*, 2238−2246.
(58) Horiki, K.; Igano, K.; Inouye, K. Amino acids and peptides. Part 6. Synthesis of the Merrifield resin esters of N-protected amino acids with the aid of hydrogen bonding. *Chem. Lett.* **1978**, *2*, 165−168.
(59) Rivier, J. E.; Jiang, G.; Porter, J.; Hoeger, C.; Craig, A. G. et al. GnRH antagonists: novel members of the azaline B family. *J. Med. Chem.* **1995**, *38*, 2649−2662.
(60) Payne, L. S.; Boger, J. Synthesis of α,Ω-diamino acids: an efficient preparation of DL-homolysine and protected derivatives. *Synth. Commun.* **1985**, *15*, 1277−1290.
(61) Cheung, S. T.; Benoiton, N. L. *N*-Methylamino acids in peptide synthesis. V. The synthesis of *N*-*tert*-butyloxycarbonyl, *N*-methylamino acids by N-methylation. *Can. J. Chem.* **1977**, *55*, 906−910.
(62) Kaiser, E.; Colescott, R. L.; Bossinger, C. D.; Cook, P. I. Color test for detection of free terminal amino groups in the solid-phase synthesis of peptides. *Anal. Biochem.* **1970**, *34*, 595−598.

JM049519M